

RIS Grouping Based Index Modulation for 6G Telecommunications

Krisma Asmoro and Soo Young Shin[✉], *Senior Member, IEEE*

Abstract—In this letter, a novel reconfigurable intelligent surface (RIS) grouping based index modulation (RGB-IM) is proposed to enhance spectral efficiency and improve bit error rate (BER). The idea is to divide an RIS into several number of group-surfaces (GR). Furthermore, the incoming data bits are modulated to spatial symbol, which represents the index of one of the available GR that will be activated at a particular time. In addition, the impact of RIS imperfect channel estimation is investigated in this letter. Both spectral efficiency and BER of the proposed system are simulated and validated with theoretical result. The computer simulation results indicate that the RGB-IM outperform a relay-assisted spatial modulation (SM).

Index Terms—Bit error rate (BER), reconfigurable intelligent surface (RIS), spectral efficiency, spatial modulation (SM).

I. INTRODUCTION

RECONFIGURABLE Intelligent Surface (RIS) key technologies for assisting wireless communication by enhancing coverage and modify the channel condition. The RIS comprises a number of low-cost elements that are capable of manipulating and modifying the incoming electromagnetic waves phases [1]. Furthermore, it is known that each part of the RIS can work independently of the others and has its own phase shifter value. Moreover, based on a channel knowledge, the RIS can be divided into two main aspects, namely intelligent and blind RIS [2]. The RIS is categorized as intelligent when the value of phase shifter is not equal to zero, means that it is modified the channel phases. On the other hand, the RIS is categorized as blind when the phase shifter is equal to zero, means that it does not have any channel information.

In the past few years, index modulation (IM) has gained popularity because of its capability to increase bits per channel usage (BPCU) by adding additional spatial symbol [3]. Receiver performs maximum likelihood (ML) detector with channel state information (CSI) to detect the transmitted spatial symbol. In [4], IM is integrated with

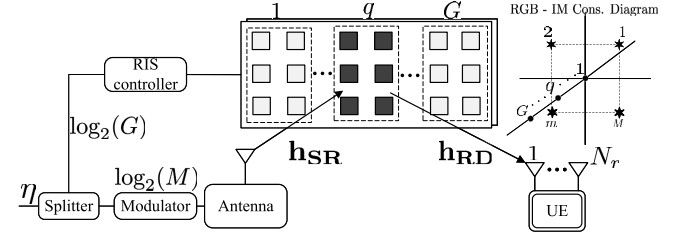


Fig. 1. Overall system model of RGB-IM.

multiple-input multiple-output orthogonal frequency-division multiplexing (MIMO-OFDM) to increase spectral efficiency. Subsequently, the RIS is deployed to aid single-input-multiple-output (SIMO) spatial modulation (SM) [5] and space shift keying (SSK) [6], [7]. In [8], with the aid of RIS, transmit and receive antenna indices were jointly modulated with user symbols. Finally, in [9] the deactivation of RIS grouping elements based space modulation is proposed to reduce error rate.

Motivated by IM techniques, the present study introduces a novel RIS grouping-based IM (RGB-IM). The main idea is to divide RIS to specific number of elements into group-surfaces. Further, the user information is split and modulated to spatial symbol which is used to activate the index of a group-surface. In this letter, it is presumed that the direct link between base station and user is not available, because the RGB-IM is aimed to enhance coverage. In contrast with previous work, the impact of imperfect RIS channel estimation is investigated. Additionally, the derived theoretical result is valid for generalized number of receive antenna and modulation level. The performance comparison of blind RIS and intelligent RIS are shown in this letter.

First, the system model of RGB-IM is introduced in Section II. The capacity and analytical bit error rates (BER) of RGB-IM is presented in Section III. Specifically, the analytical BER of blind RIS is presented in Section III-A, whereas the intelligent RIS is in Section III-B. The analytical and simulation results are presented in Section IV. Finally, the conclusions of this letter is presented in Section V.

II. SYSTEM MODEL

Fig. 1 illustrates the overall system model of the proposed RGB-IM. The RIS consists of G group-surfaces (GR) $RIS\ q \in [1, \dots, G]$. Furthermore, the receiver equipped with N_r number of receiver antennas is denoted by $r \in [1, \dots, N_r]$. The bits per channel usage (BPCU) are denoted by $\eta = \log_2(M) + \log_2(G)$, where M denotes the modulation order of the user. A bit splitter is utilized to split messages into modulator and the RIS GR activator index, denoted by x and ℓ ,

Manuscript received 26 July 2022; revised 2 September 2022; accepted 2 September 2022. Date of publication 8 September 2022; date of current version 9 November 2022. This work was supported in part by the Priority Research Centers Program through the National Research Foundation of Korea (NRF) funded by the Ministry of Education, Science and Technology under Grant 2018R1A6A1A03024003, and in part by the Ministry of Science and ICT (MSIT), South Korea, under the Grand Information Technology Research Center Support Program supervised by the Institute for Information and communications Technology Planning and Evaluation (IITP) under Grant IITP-2022-2020-0-01612. The associate editor coordinating the review of this article and approving it for publication was J. Hu. (Corresponding author: Soo Young Shin.)

The authors are with the WENS Laboratory, Department of IT Convergence Engineering, Kumoh National Institute of Technology, Gumi 39177, South Korea (e-mail: krisma@kumoh.ac.kr; wdragon@kumoh.ac.kr).

Digital Object Identifier 10.1109/LWC.2022.3205038

respectively. Furthermore, the transmitted modulated symbol is denoted as:

$$\mathbf{x}_t^{\text{RF}}(t) = \underbrace{[0 \quad \cdots \quad \cos(w_c t) \quad \cdots \quad 0]^T}_G. \quad (1)$$

The active GR comprises a finite number of elements of N_g with $i \in [1, 2, \dots, N_g]$. In this letter, we consider symmetrical configuration over sub-group RIS [10], in such that $N = N_g \times G$.¹ The channel from the single-antenna BS to the N_g number GR of RIS is denoted by \mathbf{h}_{SR} , while the channel from the RIS to cell users is denoted by \mathbf{h}_{RD} . Similar system model with [10], [11], the \mathbf{h}_{SR} is assumed to be perfect while \mathbf{h}_{RD} is imperfect. The ideal channel from RIS to user is written as:

$$\mathbf{h}_{\text{RD}} = \rho \hat{\mathbf{h}}_{\text{RD}} + \sqrt{1 - \rho^2} \Delta \mathbf{h}_{\text{RD}}, \quad (2)$$

where $\hat{\mathbf{h}}_{\text{RD}}$ is the estimated channel, ρ is the parameter of imperfect channel estimation and $\Delta \mathbf{h}_{\text{RD}} = \hat{\mathbf{h}}_{\text{RD}} - \mathbf{h}_{\text{RD}}$. The $\hat{\mathbf{h}}_{\text{RD}}$ and $\Delta \mathbf{h}_{\text{RD}}$ are mutually uncorrelated. It can be seen clearly that $\rho = 1$ denotes a perfect channel estimation while $\rho \in (0, 1)$ denotes an imperfect channel estimation.

The received signal $\mathbf{Y} = [y_1, \dots, y_r, \dots, y_{N_r}]$ at the receiver antenna can be expressed as follows:

$$\mathbf{Y} = \rho \mathbf{h}_{\text{SR}} \Phi \hat{\mathbf{h}}_{\text{RD}} x + \sqrt{1 - \rho^2} \mathbf{h}_{\text{SR}} \Phi \Delta \mathbf{h}_{\text{RD}} x + \mathbf{n}, \quad (3)$$

where $[\mathbf{h}_{\text{SR}} \in \mathbb{C}^{N_g \times 1}, \mathbf{h}_{\text{RD}} \in \mathbb{C}^{N_r \times N_g}]$ and the channels follow uncorrelated Rayleigh fading channel $C \sim \mathcal{N}(0, \sigma^2)$. In addition, $\mathbf{n} \in \mathbb{C}^{N_r \times 1}$ denotes an additive white Gaussian noise (AWGN) with a zero mean and covariance matrix of $\sigma_n^2 I_{N_r}$ (AWGN for receive antenna r is denoted by n_r). Thus, the signal-to-noise (SNR) at the receiver is given by $E_s/N_0 = 1/\sigma_n^2$. Φ denotes the RIS phase shifter, which is defined as follows:

$$\Phi = \text{diag}\{\Lambda_1 e^{j\phi_1}, \dots, \Lambda_i e^{j\phi_i}, \dots, \Lambda_N e^{j\phi_N}\}, \quad (4)$$

where Λ_i denotes the RIS element magnitude ($|\Phi| = 1$), and ϕ_i is the phase response of the RIS elements ($\angle(\Phi)$). Therefore, the received signal at receive antenna r is written as:

$$y_r = \left[\sum_{i=1}^{N_g} h_i e^{j\phi_i} \hat{g}_{r,i} \right] x + \left[\sum_{i=1}^{N_g} h_i e^{j\phi_i} \Delta g \right] x + n_r. \quad (5)$$

In Eq. (5), we assume that h_i represents the channel from BS to i^{th} RIS element, and $\hat{g}_{r,i}$ denotes the estimated channel from the i^{th} RIS element to the r receive antenna. The magnitude and channel phase of h_i and $\hat{g}_{r,i}$ are denoted as $A_i e^{j\psi_i}$ and $\hat{\beta}_{r,i} e^{j\hat{\theta}_{r,i}}$, respectively. Therefore, the value of the RIS phase is defined as $\phi_i = \psi_i + \hat{\theta}_{r,i}$. The RIS elements are utilized to minimize the channel phase. Under the given condition, the instantaneous SNR at the receive antenna r is written as follows:

$$\gamma_{\text{ins } r} = \frac{\rho^2 \left| \sum_{i=1}^{N_g} \Lambda_i A_i \hat{\beta}_{r,i} e^{j(\phi_i - \psi_i - \hat{\theta}_{r,i})} \right|^2}{(1 - \rho^2) \left| \sum_{i=1}^{N_g} \Lambda_i A_i e^{j(\phi_i - \psi_i)} \right| \kappa_{RD}^{-\tau} + \sigma_{n,r}^2}, \quad (6)$$

¹The asymmetrical element configuration is an interesting for future research direction (e.g., satisfying minimum BER or spectral efficiency demand).

where $\kappa_{RD}^{-\tau}$ denotes channel variance of \mathbf{h}_{RD} and τ denotes a path-loss exponent of it. At the receiver side, ML decoder performs joint detection for active GR RIS ℓ and modulated symbol x with an arbitrary number of N_r . Therefore, the decoded spatial symbol $\tilde{\ell}$ and the signal symbol \tilde{x} can be written as follows:

$$[\tilde{\ell}, \tilde{x}] = \arg \min_{\ell, x} \left\| \mathbf{Y} - \underbrace{\sum_{i=1}^{N_g} \left(h_{\ell,i} e^{j\phi_{\ell,i}} \hat{g}_{r,i} \right) x}_{\mathbf{H}_{\ell}} \right\|_F^2, \quad (7)$$

where $\mathbf{H} \in \mathbb{C}^{N_r \times G}$ denotes the channel estimated at the receiver, ℓ denotes its column index and $\|\cdot\|_F$ denotes Frobenius norm.

In practice, a field-programmable gate array (FPGA) can be implemented as the RIS controller, that is also works as a gateway to communicate and coordinate with other network components (e.g., BSs, APs, and user terminals) through separate wireless connections for low-rate information exchange [10], [12]. In addition, the controller holds the activator table index of sub-group RIS. Further, the FPGA can determine which index q is active according to the input from bit splitter.

III. PERFORMANCE ANALYSIS

In this section, the ergodic capacity and the analytical average bit error rate (ABER) of the proposed system are derived. In order to evaluate an ergodic capacity of SIMO and SM is written as [13]:

$$C_h = \mathbb{E} \left\{ \log_2 \left(1 + P_u \sum_{r=1}^{N_r} |h_r|^2 \right) \right\} \text{ b/s/Hz}, \quad (8)$$

where P_u denotes user SNR ($1/\sigma_n^2$). The notation b/s/Hz (bits/second/Hertz) denotes a spectral efficiency of the system. Furthermore, the ergodic capacity of RGB-IM can be expressed as:

$$C_{\text{RGB}} = \mathbb{E} \left\{ \log_2 \left(1 + P_u \sum_{r=1}^{N_r} \sum_{i=1}^{N_g} |h_i e^{j\phi_i} g_{r,i}|^2 \right) \right\}. \quad (9)$$

To derive analytical ABER of RGB-IM, we adopt pairwise error probability (PEP) [14] to calculate multiple-symbol detection symbol error probability (SEP).

A. Blind RGB-IM (B-RGB-IM)

The PEP of ML detector in Eq. (7) under the condition known as channel $\mathbf{h}_{\text{SR}}, \mathbf{h}_{\text{RD}}$ and $\Phi = 1, \phi_{\ell,i} = 0$, can be written as:

$$\begin{aligned} \text{PEP} &= \Pr((\ell, x) \rightarrow (\tilde{\ell}, \tilde{x}) \mid \mathbf{h}_{\text{SR}}, \mathbf{h}_{\text{RD}}) \\ &= Q \left(\sqrt{\frac{\left\| \sum_{i=1}^{N_g} (h_{\ell,i} \hat{g}_{r,i}) x - \sum_{i=1}^{N_g} (h_{\tilde{\ell},i} \hat{g}_{r,i}) \tilde{x} \right\|_F^2}{2\sigma_n^2}} \right) \end{aligned}$$

$$= Q\left(\sqrt{\frac{\|\mathbf{H}_\ell^b x - \mathbf{H}_\ell^b \tilde{x}\|_F^2}{2\sigma_n^2}}\right) = Q(\sqrt{v^b}), \quad (10)$$

where \mathbf{H}_ℓ^b indicates the ℓ^{th} column of the $N_r \times G$ channel matrix for blind RIS. Q denotes a Q-function defined as $Q(x) = \frac{1}{\sqrt{2\pi}} \int_x^\infty \exp(-\frac{u^2}{2}) du$. Moreover, we can write v^b as the signal-to-noise ratio (SNR) with the N_r -number antenna as:

$$v^b = \sum_{r=1}^{N_r} \gamma_r^b, \quad \text{with } \gamma_r^b = \frac{|\mathbf{H}_\ell^b x - \mathbf{H}_\ell^b \tilde{x}|^2}{2\sigma_n^2}. \quad (11)$$

In Eq. (11) indicates that v^b is the chi-squared RV [15] with a probability distribution function (PDF) of $f(v^b) = \frac{1}{\Gamma(N_r)(\bar{\gamma}^b)^{N_r}} (v^b)^{(N_r-1)} \exp(-\frac{v^b}{\bar{\gamma}^b})$. Depending on whether the spatial symbol is correctly or erroneously, the average SNR is calculated differently. Therefore, it can be expressed as follows:

$$\bar{\gamma}^b = \frac{1}{2\sigma_n^2} \times \begin{cases} |x - \tilde{x}|^2, & \text{if } \tilde{\ell} = \ell, \\ |x|^2 + |\tilde{x}|^2, & \text{if } \tilde{\ell} \neq \ell. \end{cases} \quad (12)$$

To obtain the average BER over Rayleigh fading channel, the expected value of PEP can be written as $E_v\{Q(\sqrt{v^b})\} = \int_v f(v^b) Q(\sqrt{v^b}) dv$. However, it is difficult to derive this equation. Therefore, we utilize [16] to simplify the analytical ABER bound for blind RGB-IM, which is expressed as follows:

$$\begin{aligned} \bar{P}_e^b &= \frac{1}{2\eta} \sum_{\tilde{\ell}, \tilde{x}} \sum_{\ell, x} \frac{e_{\tilde{\ell}, \tilde{x}}^{\ell, x}}{\eta} (P_{\tilde{x}})^{N_r} \\ &\times \sum_{r=0}^{N_r-1} \binom{N_r-1+r}{r} [1 - P_{\tilde{x}}]^r. \end{aligned} \quad (13)$$

The number of bits in error associated with an PEP event is denoted as $e_{\tilde{\ell}, \tilde{x}}^{\ell, x}$. The $P_{\tilde{x}}$ denotes bit error probability (BEP) of the detected symbol. The central limit theorem (CLT) is applied for a sufficient number N_g , where $N_g \gg 1$. Following aforementioned rules, the moment generating function (MGF) $\mathcal{M}_\gamma(t) = (1 - tN\gamma)^{-1}$ and the BEP binary signaling for RIS over Rayleigh fading are expressed as follows:

$$\begin{aligned} P_{\tilde{x}} &= \frac{1}{\pi} \int_0^{\pi/2} \left(\frac{1}{1 + \frac{N\bar{\gamma}}{\sin^2 \xi}} \right)^{\frac{1}{2}} d\xi \\ &= \frac{1}{2} \left(1 - \sqrt{\frac{N\bar{\gamma}/2}{1 + N\bar{\gamma}/2}} \right). \end{aligned} \quad (14)$$

B. Intelligent RGB-IM (I-RGB-IM)

In contrast to blind RIS, the phase selection of RIS is $\Phi \neq 1$. Therefore, PEP can be expressed as follows:

$$\begin{aligned} \text{PEP} &= \Pr((\ell, x) \rightarrow (\tilde{\ell}, \tilde{x}) \mid \mathbf{h}_{\text{SR}}, \mathbf{h}_{\text{RD}}) \\ &= \Pr(\|\mathbf{Y} - \mathbf{H}_\ell^{\text{In}} x\|_F^2 > \|\mathbf{Y} - \mathbf{H}_{\tilde{\ell}}^{\text{In}} \tilde{x}\|_F^2) \end{aligned}$$

$$= Q\left(\sqrt{\frac{\|\mathbf{H}_\ell^{\text{In}} x - \mathbf{H}_{\tilde{\ell}}^{\text{In}} \tilde{x}\|_F^2}{2\sigma_n^2}}\right) = Q(\sqrt{v^{\text{In}}}), \quad (15)$$

where the received signal is $\mathbf{H}_\ell^{\text{In}} = \sum_{i=1}^{N_g} h_{\ell,i} e^{j\phi_{\ell,i}} \hat{g}_{r,i}$. Under the detected condition, the received signal is $\tilde{\ell}$, and \tilde{x} is $\mathbf{H}_{\tilde{\ell}}^{\text{In}} = \sum_{i=1}^{N_g} h_{\tilde{\ell},i} e^{j\phi_{\tilde{\ell},i}} \hat{g}_{r,i}$. In addition, we can define an average receive SNR of v^{In} using Eq. (11). The average PEP (APEG) under the fading channel for M-QAM modulation of the Q-function of intelligent MGF $\mathcal{M}_{v^{\text{In}}}$ can be expressed as [15]:

$$\begin{aligned} P_{\tilde{x}} &= \frac{4}{\pi} \left(1 - \frac{1}{\sqrt{M}} \right) \int_0^{\pi/2} \mathcal{M}_{v^{\text{In}}} \left(-\frac{\lambda}{\sin^2 \phi} \right) d\phi \\ &- \frac{4}{\pi} \left(1 - \frac{1}{\sqrt{M}} \right)^2 \int_0^{\pi/4} \mathcal{M}_{v^{\text{In}}} \left(-\frac{\lambda}{\sin^2 \phi} \right) d\phi, \end{aligned} \quad (16)$$

where $\lambda = 1.5(M-1)^{-1}$, and $\mathcal{M}_{v^{\text{In}}}$ is the MGF of Eq. (15). Based on Eq. (6), A_i and $\beta_{r,i}$ are Rayleigh distributed random variables (RV). Therefore, its mean can be written as $E[A_i \beta_{r,i}] = \mu_v = N \frac{\pi}{4}$ and the variance as $\text{VAR}[A_i \beta_{r,i}] = \sigma_v^2 = N \frac{16-\pi^2}{8}$. Consider an MGF model from [17] with n degrees of freedom (DoF), which can be written as:

$$\mathcal{M}_{v^{\text{In}}}(s) = \left(\frac{1}{\sqrt{1 - 2s\sigma_v^2}} \right)^{n/2} \exp\left(\frac{s\mu_v^2}{1 - 2s\sigma_v^2} \right). \quad (17)$$

In contrast to blind RIS, the average received SNR cannot be defined using Eq. (11). In this case, we utilize the MGF from Eq. (17) and define MGF for two cases $\tilde{\ell} = \ell \rightarrow \mathcal{M}_{\tilde{\gamma}}^{\text{cor}}$, $\tilde{\ell} \neq \ell \rightarrow \mathcal{M}_{\tilde{\gamma}}^{\text{inc}}$.

Let $u(\tilde{\ell}, \ell)$ be a square norm Euclidean distance $|\tilde{\ell} - \ell|^2$. Accordingly, the MGF for correct detection of the RIS group index $\tilde{\ell} = \ell$ is written as follows:

$$\mathcal{M}_{\tilde{\gamma}}^{\text{cor}}(t) = \left(\frac{1}{1 - \frac{tN(16-\pi^2)u(\tilde{\ell}, \ell)}{8}} \right)^{\frac{1}{2}} \exp\left(\frac{\frac{tN^2\pi^2 u(\tilde{\ell}, \ell)}{16}}{1 - \frac{tN(16-\pi^2)u(\tilde{\ell}, \ell)}{8}} \right). \quad (18)$$

To estimate the MGF while $\tilde{\ell} \neq \ell$, we first define the transmitted symbol as $x = x_{\Re} + j x_{\Im}$ and the decoded symbol as $x = \tilde{x}_{\Re} + j \tilde{x}_{\Im}$ for M-QAM modulation. Here, the decision on $\tilde{\ell}$, obtained from Eq. (15), we rewrite PEP as:

$$\Pr(\ell \rightarrow \tilde{\ell} \mid x) = \Pr\left(\underbrace{Z_1^2 + Z_2^2 - Z_3^2 - Z_4^2}_{\mathbf{Z}} < 0 \right), \quad (19)$$

where $Z_1 = (\mathbf{H}_\ell^{\text{In}} + \mathbf{n})_{\Re}$, $Z_2 = (\mathbf{H}_\ell^{\text{In}} + \mathbf{n})_{\Im}$, $Z_3 = (\mathbf{H}_{\tilde{\ell}}^{\text{In}} + \mathbf{n})_{\Re}$, and $Z_4 = (\mathbf{H}_{\tilde{\ell}}^{\text{In}} + \mathbf{n})_{\Im}$. Furthermore, \mathbf{Z} follows a Gaussian distribution, and Z_1 and Z_2 are correlated, because of the non-zero values of (x_{\Re}, x_{\Im}) . Therefore, a quadratic form of RV approach is required to derive the MGF of \mathbf{Z} . The MGF of Gaussian quadratic RV is denoted as [18]:

$$\begin{aligned} \mathcal{M}_{\tilde{\gamma}}^{\text{inc}}(t) &= \det(\mathbf{I} - 2t\mathbf{A}\mathbf{\Sigma})^{-\frac{1}{2}} \\ &\times \exp\left\{ -\frac{1}{2} \mathbf{\Omega}^T [\mathbf{I} - (\mathbf{I} - 2t\mathbf{A}\mathbf{\Sigma})^{-1}] \mathbf{\Sigma}^{-1} \mathbf{\Omega} \right\}, \end{aligned} \quad (20)$$

where $\mathbf{A} = \mathbf{I}$ and \mathbf{I} is an identity matrix with 4×4 size. Consider $\mathbf{Z} = \mathbf{c}^T \mathbf{A} \mathbf{c}$ for $\mathbf{c} = [Z_1 \ Z_2 \ Z_3 \ Z_4]^T$. The expected value $E[\mathbf{Z}]$, can be written as follows:

$$\mathbf{\Omega} = \begin{bmatrix} \frac{N\pi x_{\Re}}{4} & \frac{N\pi x_{\Im}}{4} & -\frac{N\pi \tilde{x}_{\Re}}{4} & -\frac{N\pi \tilde{x}_{\Im}}{4} \end{bmatrix}. \quad (21)$$

Furthermore, the covariance of \mathbf{Z} is expressed as follows:

$$\text{Cov}(\mathbf{Z}) = \mathbf{\Sigma} = \begin{bmatrix} \sigma_1^2 & \sigma_{1,2} & \sigma_{1,3} & \sigma_{1,4} \\ \sigma_{2,1} & \sigma_2^2 & \sigma_{2,3} & \sigma_{2,4} \\ \sigma_{3,1} & \sigma_{3,2} & \sigma_3^2 & \sigma_{3,4} \\ \sigma_{4,1} & \sigma_{4,2} & \sigma_{4,3} & \sigma_4^2 \end{bmatrix},$$

$$\sigma_1^2 = \frac{N(16-\pi^2)}{8} x_{\Re}^2 + \frac{N|\tilde{x}|^2}{2}, \quad \sigma_2^2 = \frac{N(16-\pi^2)}{8} x_{\Im}^2 + \frac{N|\tilde{x}|^2}{2},$$

$$\sigma_3^2 = \frac{N(16-\pi^2)}{8} \tilde{x}_{\Re}^2 + \frac{N|x|^2}{2}, \quad \sigma_4^2 = \frac{N(16-\pi^2)}{8} \tilde{x}_{\Im}^2 + \frac{N|x|^2}{2},$$

$$\sigma_{1,2} = \frac{N(16-\pi^2)}{8} x_{\Re} x_{\Im}, \quad \sigma_{3,4} = \frac{N(16-\pi^2)}{8} \tilde{x}_{\Re} \tilde{x}_{\Im},$$

$$\sigma_{1,3} = \frac{N(\pi^2-4\pi)}{8} (-x_{\Re} \tilde{x}_{\Re} + x_{\Im} \tilde{x}_{\Im}), \quad \sigma_{2,4} = -\sigma_{1,3},$$

$$\sigma_{1,4} = -\frac{N(\pi^2-4\pi)}{8} (x_{\Re} \tilde{x}_{\Im} + \tilde{x}_{\Re} x_{\Im}), \quad \sigma_{2,3} = \sigma_{1,4}.$$

Finally, the generalized case (arbitrary number of N and N_r) union bound ($P_{sim} \leq \bar{P}_e^{In}$) for analytical BER of intelligent RGB-IM is written as:

$$P_{sim} \leq \frac{1}{MN_r} \sum_{\ell} \sum_{\tilde{\ell}} \sum_x \sum_{\tilde{x}} \frac{\bar{P}_x(\ell, x \rightarrow \tilde{\ell}, \tilde{x}) e_{\ell, \tilde{\ell}}^{\ell, l}}{\eta}. \quad (22)$$

The derived analytical result can be implemented in far-field type RIS [19] and the index modulation with M-QAM modulation [20]. Therefore, it is feasible to implement it on the field with calculated union bound of BER. However, the main challenge is that in this letter, we consider a continuous phase for RIS which is harder to implement than the discrete [21].

IV. NUMERICAL RESULTS

In this section, the simulation and analytical graphs are shown to validate the proposed system. Specifically, the theoretical and analytical ABER union bounds of the proposed system are discussed. For the sake of fair comparison, we compare our proposed system with similar dual-hop communication scenario, namely amplify forward (AF) and full duplex decode forward (DF) relay assisted spatial modulation (AF-SM and DF-SM). Similar setup with [22] where relay AF-SM is equipped with single antenna receiver and transmitter, while relay DF-SM has N_r receiver and N_t transmitter.

Fig. 2 shows a comparison between I-RGB-IM and B-RGB-IM. As expected, for RGB-IM simulation, the results follow theoretical bounds derived in Section III. Specifically, it is aligned with analytical result for higher SNR and higher elements number. In the same manner B-RGB-IM simulations follow the theoretical results. Compared to B-RGB-IM, I-RGB-IM exhibits more performance.

Fig. 3 depicts the impact of imperfect CSI to the proposed system. The perfect CSI case ($\rho = 1$, $Ng = 4$) causing the ABER is decreasing for higher SNR. However, when the ρ is 0.8, the channel estimation is becoming imperfect. Therefore, the error floors is occurring. The B-RGB-IM with lower elements are suffering with higher error floor for $\rho = 0.8$. In order

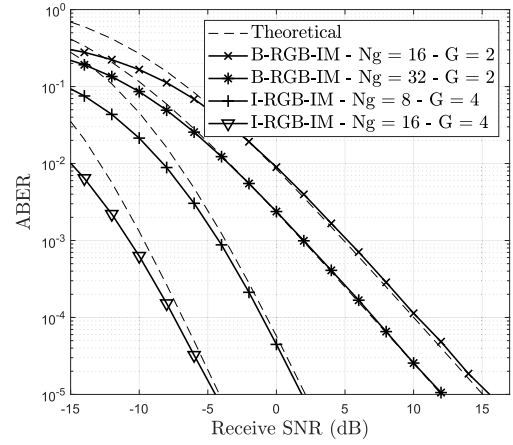


Fig. 2. The ABER performance comparison of I-RGB-IM and B-RGB-IM over different number of Ng .

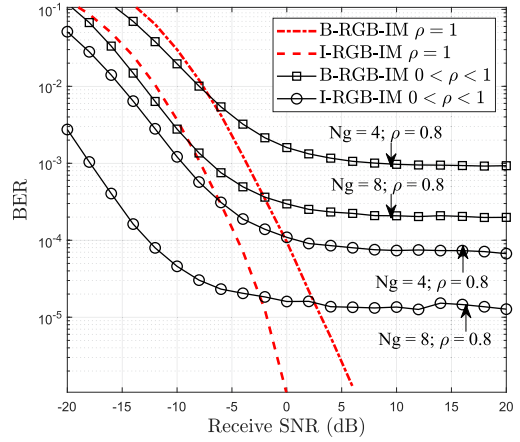


Fig. 3. The ABER performance of the proposed system with various number of elements and $0 < \rho < 1$.

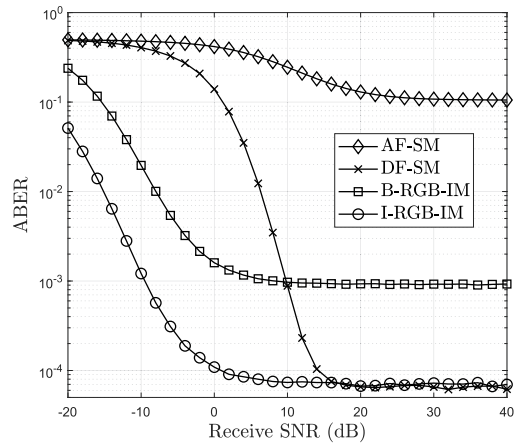


Fig. 4. The ABER performance comparison between RGB-IM and relay assisted SM with $\rho = 0.8$.

to reduce the ABER, number of elements per group have to be increased.

Fig. 4 depicts the superiority of the proposed system over imperfect CSI ($\rho = 0.8$). In this scenario, RGB-IM perform

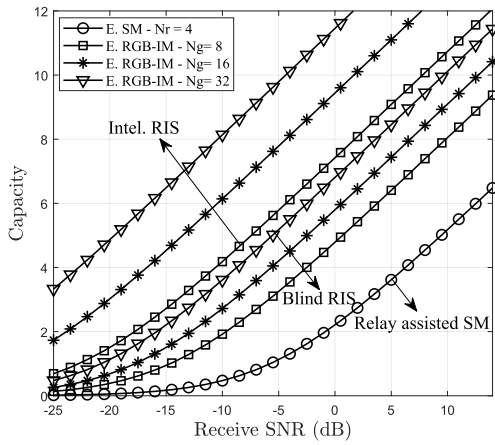


Fig. 5. Ergodic capacity of proposed system and Relay-Assisted SM.

better than relaying system with $N_g = 4$. The DF-SM is outperforming B-RGB-IM. At the same time, DF-SM has a lower ABER performance than I-RGB-IM (10^{-4} at 16 dB).

Fig. 5 shows ergodic capacity obtained from Eq. (9). In this scenario, the parameter of the simulation is determined as follows: $G = 4$, $N_g \in [8, 16, 32]$. As expected, the proposed system is performing better with larger N_g . The intelligent RIS gains significant performance with higher number of elements compare to relay assisted SM system.

V. CONCLUSION

In this letter, a novel RGB-IM is proposed and evaluated using capacity and ABER simulations that were verified with mathematical model, to measure its superiority for 6G Telecommunications. The results reveal that RGB-IM is capable of downscaling the error probability for a low received SNR. Moreover, both blind and intelligent RGB-IM provide better error performance than a relay assisted SM system. However, the trade-off of the proposed system is that, the ergodic capacity is lower than a conventional RIS that utilized all elements. In exchange of the trade-off, the RGB-IM provides more BPCU than RIS without activation IM grouping technique. The exploration of highly correlated spatial channel model, different channel fading types, and quadrature-based space modulation are interesting for future research directions.

REFERENCES

[1] E. Basar, "Transmission through large intelligent surfaces: A new frontier in wireless communications," in *Proc. Eur. Conf. Netw. Commun. (EuCNC)*, 2019, pp. 112–117.

[2] E. Basar, M. Di Renzo, J. De Rosny, M. Debbah, M.-S. Alouini, and R. Zhang, "Wireless communications through reconfigurable intelligent surfaces," *IEEE Access*, vol. 7, pp. 116753–116773, 2019.

[3] T. Mao, Q. Wang, Z. Wang, and S. Chen, "Novel index modulation techniques: A survey," *IEEE Commun. Surveys Tuts.*, vol. 21, no. 1, pp. 315–348, 1st Quart., 2019.

[4] S. Gao, M. Zhang, and X. Cheng, "Precoded index modulation for multi-input multi-output OFDM," *IEEE Trans. Wireless Commun.*, vol. 17, no. 1, pp. 17–28, Jan. 2018.

[5] E. Basar, "Reconfigurable intelligent surface-based index modulation: A new beyond MIMO paradigm for 6G," *IEEE Trans. Commun.*, vol. 68, no. 5, pp. 3187–3196, May 2020.

[6] A. E. Canbilen, E. Basar, and S. S. Ikki, "Reconfigurable intelligent surface-assisted space shift keying," *IEEE Wireless Commun. Lett.*, vol. 9, no. 9, pp. 1495–1499, Sep. 2020.

[7] Q. Li, M. Wen, S. Wang, G. C. Alexandropoulos, and Y.-C. Wu, "Space shift keying with reconfigurable intelligent surfaces: Phase configuration designs and performance analysis," *IEEE Open J. Commun. Soc.*, vol. 2, pp. 322–333, 2021.

[8] T. Ma, Y. Xiao, X. Lei, P. Yang, X. Lei, and O. A. Dobre, "Large intelligent surface assisted wireless communications with spatial modulation and antenna selection," *IEEE J. Sel. Areas Commun.*, vol. 38, no. 11, pp. 2562–2574, Nov. 2020.

[9] Y. Hussein, M. Assaad, and H. Sari, "Reconfigurable intelligent surface index modulation with signature constellations," in *Proc. IEEE Wireless Commun. Netw. Conf. (WCNC)*, 2021, pp. 1–7.

[10] C. You, B. Zheng, and R. Zhang, "Channel estimation and passive beamforming for intelligent reflecting surface: Discrete phase shift and progressive refinement," *IEEE J. Sel. Areas Commun.*, vol. 38, no. 11, pp. 2604–2620, Nov. 2020.

[11] P. Yang, L. Yang, and S. Wang, "Performance analysis for RIS-aided wireless systems with imperfect CSI," *IEEE Wireless Commun. Lett.*, vol. 11, no. 3, pp. 588–592, Mar. 2022.

[12] Q. Wu and R. Zhang, "Towards smart and reconfigurable environment: Intelligent reflecting surface aided wireless network," *IEEE Commun. Mag.*, vol. 58, no. 1, pp. 106–112, Jan. 2020.

[13] D. Gesbert, M. Shafi, D.-S. Shiu, P. Smith, and A. Naguib, "From theory to practice: An overview of MIMO space-time coded wireless systems," *IEEE J. Sel. Areas Commun.*, vol. 21, no. 3, pp. 281–302, Apr. 2003.

[14] R. Mesleh and A. Alhasssi, *Space Modulation Techniques*. Hoboken, NJ, USA: Wiley, May 2018.

[15] M. K. Simon and M.-S. Alouini, *Digital Communication Over Fading Channels*. Hoboken, NJ, USA: Wiley, 2005.

[16] M.-S. Alouini and A. J. Goldsmith, "A unified approach for calculating error rates of linearly modulated signals over generalized fading channels," *IEEE Trans. Commun.*, vol. 47, no. 9, pp. 1324–1334, Sep. 1999.

[17] J. G. Proakis, *Digital Communications*, 5th ed. Boston, MA, USA: McGraw-Hill, 2007.

[18] A. M. Mathai and S. B. Provost, *Quadratic Forms in Random Variables: Theory and Applications* (Statistics: A Series of Textbooks and Monographs), 1st ed. Boca Raton, FL, USA: CRC Press, 1992.

[19] X. Wei, L. Dai, Y. Zhao, G. Yu, and X. Duan, "Codebook design and beam training for extremely large-scale RIS: Far-field or near-field?" *China Commun.*, vol. 19, no. 6, pp. 193–204, Jun. 2022.

[20] S. Gokceli, E. Basar, M. Wen, and G. K. Kurt, "Practical implementation of index modulation-based waveforms," *IEEE Access*, vol. 5, pp. 25463–25473, 2017.

[21] X. Wang, Z. Fei, J. Huang, and H. Yu, "Joint waveform and discrete phase shift design for RIS-assisted integrated sensing and communication system under Cramer-Rao bound constraint," *IEEE Trans. Veh. Technol.*, vol. 71, no. 1, pp. 1004–1009, Jan. 2022.

[22] Q. Li, M. Wen, M. D. Renzo, H. V. Poor, S. Mumtaz, and F. Chen, "Dual-hop spatial modulation with a relay transmitting its own information," *IEEE Trans. Wireless Commun.*, vol. 19, no. 7, pp. 4449–4463, Jul. 2020.